Mutations of the Ephrin-B1 Gene Cause Craniofrontonasal Syndrome

Ilse Wieland,[1] Sibylle Jakubiczka,[1] Petra Muschke,[1] Monika Cohen,[3] Hannelore Thiele,[4] Klaus L. Gerlach,[2] Ralf H. Adams,[5] and Peter Wieacker[1]

[1]Institut für Humangenetik, and [2]Klinik für Mund-, Kiefer- und Gesichtschirurgie, Otto-von-Guericke-Universität Magdeburg, Magdeburg, Germany; [3]Medizinische Genetik, im Kinderzentrum München, München, Germany; [4]Institut für Humangenetik, Martin-Luther-Universität Halle, Halle, Germany; and [5]Cancer Research UK London Research Institute, London, United Kingdom

Craniofrontonasal syndrome (CFNS) is an X-linked craniofacial disorder with an unusual manifestation pattern, in which affected females show multiple skeletal malformations, whereas the genetic defect causes no or only mild abnormalities in male carriers. Recently, we have mapped a gene for CFNS in the pericentromeric region of the X chromosome that contains the *EFNB1* gene, which encodes the ephrin-B1 ligand for Eph receptors. Since *Efnb1* mutant mice display a spectrum of malformations and an unusual inheritance reminiscent of CFNS, we analyzed the *EFNB1* gene in three families with CFNS. In one family, a deletion of exons 2–5 was identified in an obligate carrier male, his mildly affected brother, and in the affected females. In the two other families, missense mutations in *EFNB1* were detected that lead to amino acid exchanges P54L and T111I. Both mutations are located in multimerization and receptor-interaction motifs found within the ephrin-B1 extracellular domain. In all cases, mutations were found consistently in obligate male carriers, clinically affected males, and affected heterozygous females. We conclude that mutations in *EFNB1* cause CFNS.

Introduction

Craniofrontonasal syndrome (CFNS [MIM 304110]), a subgroup of craniofrontonasal dysplasia, is characterized by craniofacial asymmetry, hypertelorism, coronal synostosis, strabismus, bifid nasal tip, grooved nails, and abnormalities of the thoracic skeleton, as well as wiry and curly hair. Rare manifestations are anterior cranium bifidum, axillary pterygium, joint abnormalities, cleft lip and palate, unilateral breast hypoplasia, asymmetric lower-limb shortness, corpus callosum hypoplasia, umbilical hernia, and diaphragmatic hernia. CFNS shows a very unusual pattern of X-linked inheritance, in which most affected patients are females and obligate male carriers show no or only mild manifestation, such as hypertelorism (Saavedra et al. 1996). Compagni et al. (2003) reported that targeted inactivation of the X-linked gene *Efnb1* in mice causes partial perinatal lethality, abdominal wall closure defects, and skeletal abnormalities, especially of the thoracic cage. Interestingly, the phenotype was more severe in female heterozygotes than in hemizygous males, and some defects, such as preaxial polydactyly, were only detected in heterozygotes. The human homologue *EFNB1* (MIM 300035)

is localized at Xq12, within the mapping interval for CFNS (DXS993/PFC–DXS1125/DXS8111) (Wieland et al. 2002), making *EFNB1* a striking candidate gene for this syndrome. However, locus heterogeneity for CFNS cannot be excluded, because previous linkage studies suggested a localization of CFNS in Xp22 (Feldman et al. 1997).

Subjects and Methods

Patients and Study Subjects

All members of the families included in this study gave their informed consent to perform linkage and haplotype analysis as well as to search for mutations in candidate genes. The affected females exhibit typical features of CFNS, including hypertelorism and craniofacial abnormalities, such as orbital asymmetry (fig. 1). All affected females of these three families are normal in their mental performance and show no behavioral abnormalities. Body height is also in the normal range for all affected females.

The pedigree of family 1 is shown in figure 2A. In patient III1, hypertelorism, bifid nasal tip, grooved nails, axillary pterygium, and slight pterygium colli were observed. In I2 and II6, hypertelorism and grooved nails have been reported. The obligate male carrier (II3) and his brother (II5) show only hypertelorism as a microsymptom of CFNS.

The pedigree of family 2 is shown in figure 3A. The phenotypes of the patients include hypertelorism, orbital asymmetry, brachycephaly, brachydactyly, and Sprengel

Figure 1   Orbital asymmetry in a patient with CFNS

deformity. In III6, who experienced four miscarriages at mid-pregnancy, uterus arcuatus has been detected. In addition, III6 has curly hair as well as grooved finger nails and unilateral breast hypoplasia. The obligate carrier male (III2) shows no phenotypic abnormalities. The son (V3) of an affected female exhibits a broad nasal bridge, with an inner canthel distance of 3.8 cm, at 9 years of age.

The pedigree of family 3 is shown in figure 4*A*. I1 shows a slight facial asymmetry and a broad nasal bridge. In II1, severe facial asymmetry, hypertelorism, and hypoplasia of corpus callosum were observed. Her daughter (III2) exhibits facial asymmetry, hypertelorism, agenesis of the corpus callosum, complete syndactyly of the third and fourth finger on the left side, and scoliosis. Her son (III1) exhibits no features of CFNS.

Genotyping, X-Inactivation Test, and Candidate Gene Analysis

Haplotype analysis of families 1 and 3 with the use of microsatellite markers from chromosome X was performed as described elsewhere (Wieland et al. 2002). To control for the pattern of X inactivation, the HUMAR assay (Allen et al. 1992) was applied as described elsewhere (Wieland et al. 2002). Deletion analysis of the *EFNB1* gene was performed by PCR with the use of primers 5′-GGCAGAGGAAGGCGAGGCGA-3′ and 5′-CAACCCAGCCAAGTGCCCCT-3′, which generated a 401-bp PCR product from exon 1; primers 5′-GGCTCT-TGTCCGCTTCCCTG-3′ and 5′-AGAGGATGGGGATG-
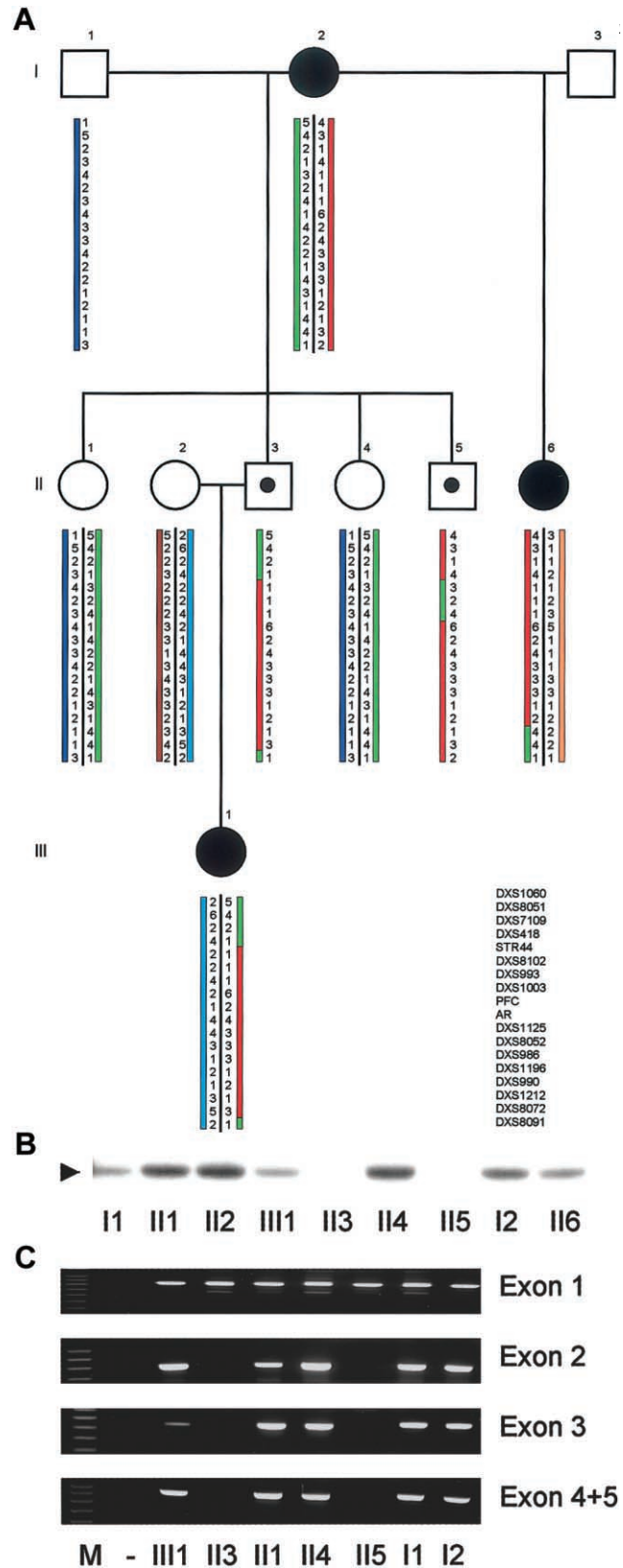
Figure 2   Family 1. *A*, Pedigree of family 1 with CFNS. *B*, Deletion of the *EFNB1* gene in family 1, detected by Southern blot analysis using exon 2 of the *EFNB1* gene as a probe. *C*, PCR analysis of exons 1–5 of *EFNB1*. Lane numbers refer to family members depicted in the pedigree.

A

B

C

IV3 III2 IV1 IV2 V1 V2 V3 II1 III6 II4
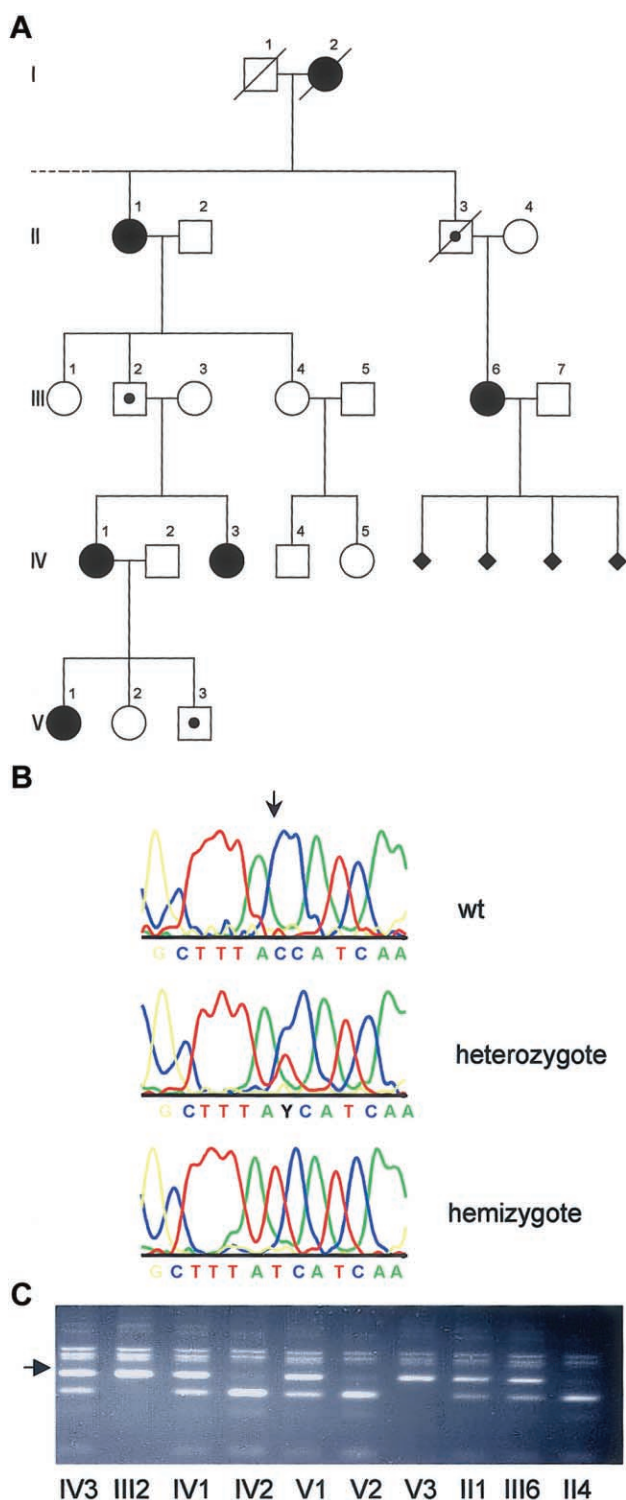
Figure 3 Family 2. *A*, Part of the pedigree of family 2. *B*, Missense mutation 1023C→T in exon 2 of *EFNB1* in the hemizygous obligate carrier male (III2) and in an affected heterozygous female. *C*, PCR analysis and *Rsa*I restriction enzyme cleavage of exon 2 of *EFNB1*. Lane numbers refer to family members depicted in the pedigree, and the fragments carrying the mutation are indicated by an arrow.

GGCGG-3′, which generated a 386-bp PCR product from exon 2; and primers 5′-GGGGAGCAGGCGTAG-GGTTA-3′ and 5′-GCAAGGGGAGGGGGTGTG-3′, which generated an 892-bp PCR product from exons 4 and 5. PCR products were analyzed by agarose gel electrophoresis. For sequence analysis, PCR products were isolated by gel extraction (QiaExII, Qiagen) and cloned into vector pCR2.1, as recommended by the supplier (Invitrogen). Plasmid preparations of single colonies were analyzed by M13 sequencing on an automatic laser fluorescent (ALF) express sequencer (Pharmacia). At least two independent clones were sequenced. For direct patient-DNA sequencing, Cy5-labeled exon-specific *EFNB1* primers were used (table 1 [online only]). Standard sequencing reactions were performed using a kit (Amersham-Biotech) and were resolved on an ALF express sequencer (Pharmacia). Sequences were analyzed by DNAsis (Hitashi).

For analysis of DNA from normal controls and from family members of the pedigrees, standard PCR was performed using primers for exon 2 of the *EFNB1* gene, as described above. The PCR products were digested with *Bsl*I (New England BioLabs) to control for 862T→C. PCR products from the wild type generated fragments of 24 bp, 97 bp, 126 bp, and 139 bp. PCR products containing 862T→C generated fragments of 24 bp, 126 bp, and 236 bp. To control for missense mutation 1023T→C, PCR products from exon 2 were reamplified with the use of primers 5′-CCTGCAATAGGCCAGAG-CAGGAAATACGCTGT-3′, which introduces an *Rsa*I restriction-enzyme site specifically at 1023T, and 5′-GGATGGGATGGGCGGGACTCACAG-3′. PCR and cleavage products were analyzed on 3% agarose gels.

Southern Blot Hybridization

High molecular-weight patient DNA was cleaved with restriction endonuclease *Pst*I (New England BioLabs). The digests were resolved on an 0.8% agarose gel and were blotted on Nylon membrane (Hybond-N+, Amersham Biosciences). Hybridization probes for *EFNB1* exon 2 were prepared from PCR products (described above) and were radiolabeled by random priming using α[³²P] dCTP. Hybridization, washings, and autoradiography were performed in accordance with standard protocols (Sambrook et al. 1989).

Results

Haplotype analysis in family 1 (fig. 2*A*), with the use of 18 informative, polymorphic DNA markers, confirmed our previous mapping interval in the pericentromeric region of the X chromosome that contains the *EFNB1* gene. The *EFNB1* gene comprises 13.17 kb and 5 exons (LocusLink accession number 1947; Ensembl accession
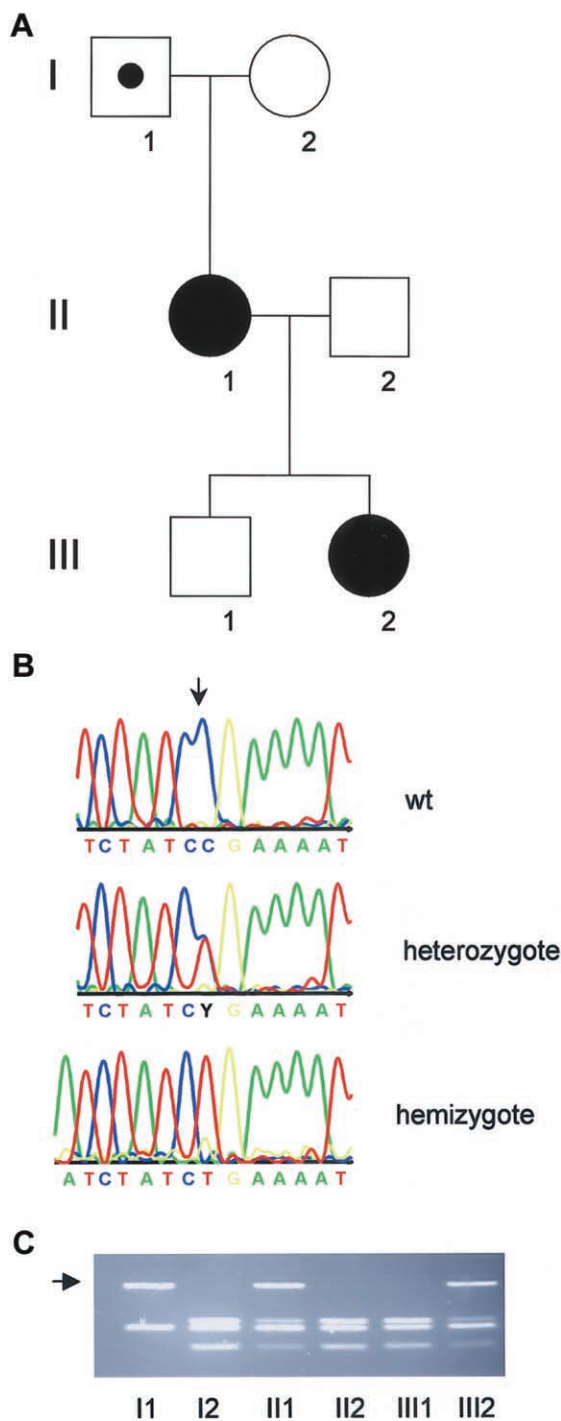
Figure 4 Family 3. *A,* Part of the pedigree of family 3. *B,* Missense mutation 862C→T in the hemizygous affected male (I1) and in a heterozygous affected female (III2) of pedigree 3. *C,* PCR-based detection of the 862C→T mutation in family 3. Lane numbers refer to family members depicted in the pedigree, and the fragments carrying the mutation are indicated by an arrow.

number ENSP00000204961). In this family, a deletion of exons 2–5 of the *EFNB1* gene was detected in the obligate male carrier (II3) and in his mildly affected brother (II5) by PCR and Southern blot analysis (fig. 2*B* and 2*C*). The distal deletion breakpoint was located between markers *RH65456* and *DXS981*, suggesting a deletion of a minimum 29 kb and a maximum 148 kb. Although exon 1 is not deleted, production of a functional protein from this allele is not expected, since exon 1 merely encodes the signal peptide and 13 additional amino acids of the ephrin-B1 protein. Deletion of exon 2 was not detected in 100 male controls analyzed by PCR (data not shown). Semiquantitative Southern blot analysis, with the use of exon 2 of the *EFNB1* gene as hybridization probe, revealed half the gene dosage in the affected females, compared with unaffected female relatives (fig. 2*B*).

In family 2 (fig. 3*A*), DNA sequencing of the coding region of exons 1–5 of the *EFNB1* gene revealed the hemizygous missense mutation 1023C→T (with the use of *EFNB1* reference sequence [GenBank accession number XM_038809]) in exon 2 in the obligate male carrier, III2 (fig. 3*B*). All affected females in this family were heterozygous for 1023C→T. Furthermore, a heterozygous female's son (V3), clinically identified as an affected male because of hypertelorism, also carries this mutation (fig. 3*C*).

In family 3 (fig. 4*A*), mapping information for the CFNS locus was not available, because haplotype analysis was not informative (data not shown). The carrier male (I1) harbored the missense mutation 862C→T in exon 2 (fig. 4*B*) and the two affected females (II1 and III2) were heterozygous (fig. 4*C*). Both of the identified missense mutations have not been recorded as allele variants in the databases (GenBank and dbSNP) and were not detected in 150 control X chromosomes (data not shown). 1023C→T replaces Thr 111 with Ile, and 862C→T replaces Pro 54 with Leu, in the extracellular domain of ephrin-B1 (fig. 5*A*). Both Thr 111 and Pro 54 are highly conserved in the three known ephrin-B ligands and across a great variety of species (fig. 5*B*). Therefore, we assume that both mutations will compromise the biological activity of ephrin-B1. In all affected females of the three families, no skewed inactivation of the X chromosome was detected by the HUMAR assay (data not shown).

Discussion

Ephrin ligands and Eph-receptor tyrosine kinases are versatile regulators of embryonic tissue morphogenesis, with known functions in many tissues and organ systems (Wilkinson 2001; Kullander and Klein 2002). The eight known ephrin-ligands are divided into the ephrin-A ligands (EFNA1–A5), which are membrane anchored by
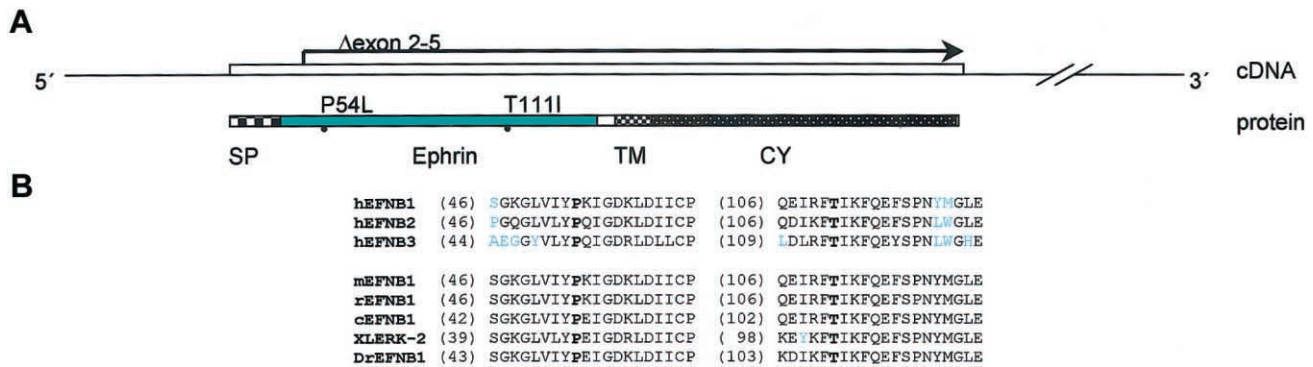
Figure 5 EFNB1 protein and ephrin-B conservation. *A,* Position of *EFNB1* missense mutations that cause CFNS. The mutations are shown on the primary sequence of EFNB1 protein with its signal peptide (SP), transmembrane domain (TM), and cytoplasmic domain (CY). Both missense mutations are located in the ephrin extracellular domain. Deletion Δexon 2–5 is indicated at the cDNA level. *B,* Evolutionary conservation of P54 and T111 in the ephrin-B class. Domains containing P54 (*left column of amino acids*) and T111 at the G-H loop (Himanen et al. 2001; Toth et al. 2001) (*right column of amino acids*) of human EFNB1-B3 and of EFNB1 protein from mouse (m), rat (r), chicken (c), frog (X), and zebrafish (Dr) are shown.

a glycosylphosphatidylinositol linkage, and ephrin-B ligands (EFNB1–B3), which are transmembrane proteins. The 14 known ephrin-receptors in vertebrates can be divided into two subclasses, EphA and EphB receptors, depending on their preferential affinity to ephrin-A or ephrin-B proteins (Kullander and Klein 2002). EphB receptors signal in combination with B-class ephrins to control the patterning of the developing skeleton, the nervous system, the intestine, and the blood vessels. It is noteworthy that ephrins not only function as ligands but also exhibit receptor-like effects (Wilkinson 2001). The Eph/ephrin transduction system plays a role in the guidance of neuronal growth and cell migration, mainly by providing repulsive signals (Murai and Pasquale 2003).

Ephrin-B1 mutant mice display malformations of the axial and appendicular skeleton, such as asymmetric attachment of ribs, lack of joints, and polydactyly. These defects have been attributed to missing or ectopic segmentation of mesenchymal condensations during early steps of skeletal development (Compagni et al. 2003). Patients with CFNS show striking asymmetry of craniofacial structures and other skeletal malformations. Abnormalities of the thoracic skeleton in CFNS include Sprengel deformity, clavicle pseudoarthrosis, pectus excavatum, and disorders of ribs and sternum that are similar to the defects observed in ephrin-B1 knockout mice. Other CNFS features are midline defects, including anterior cranium bifidum, corpus callosum hypoplasia, cleft lip and palate, omphalocele, and diaphragma hernia. In this context, it is interesting that, in family 2, one affected female who had four miscarriages at mid-pregnancy exhibits a uterus arcuatus. This malformation, caused by a failure of the fusion of the Müllerian derivatives, would explain the higher risk of abortion observed in some women affected by CFNS

(Devriendt et al. 1995). Many of these malformations show significant similarity to malformations in mice lacking ephrin-B1 or EphB receptors (Henkemeyer et al. 1996; Orioli et al. 1996; Compagni et al. 2003).

Our results demonstrate unambiguously that mutations of *EFNB1* cause CFNS. At the molecular level, deletion of the *EFNB1* gene in family 1 is most similar to target inactivation of *Efnb1* in the mouse. Missense mutations T111I and P54L in the two other families appear to abrogate ephrin-B1–Eph receptor binding. Elsewhere, crystal-structure analysis of the highly related ephrin-B2 ligand showed that the corresponding Thr of ephrin-B2 is one of the crucial residues at the G-H loop involved in ligand dimerization and Eph receptor binding (Himanen et al. 2001; Toth et al. 2001). These processes are thought to be highly relevant for interactions with Eph receptors and signaling processes, which can be blocked by mimetic peptides of the ephrin G-H loop (Koolpe et al. 2002).

The unusual pattern of manifestation of CFNS— multiple skeletal malformations in affected females and no or mild malformations in male carriers—may be explained by the promiscuity of ephrin receptors and their ligands and as the consequence of random X inactivation in females. The *EFNB1* gene is subjected to X inactivation (Carrel et al. 1999), and there is no evidence for a homologous gene on the Y chromosome (LocusLink). The HUMAR assay, performed on lymphocyte DNA of all affected females of the three families, revealed a random X inactivation. Furthermore, Compagni et al. (2003) have shown that *Efnb1* mutant female mice are mosaic for Efnb1-positive and Efnb1-negative cell clones. These experimental data and the clinical observations of the marked phenotype in heterozygotes and of the absent or mild manifestation in hemizygotes strongly support the idea that a skewed X inactivation

is not the cause of the sex-dependent manifestation of this syndrome. In fact, we expect that a random X inactivation has an implication for the manifestation of CFNS. Because ephrins are expressed in a complex, spatially and temporally dynamic pattern during embryogenesis, we assume that, in heterozygous females, ephrin-B1–expressing and ephrin-B1–deficient cells lead to divergent cell sorting and migration. This disturbance could be more pronounced in the contact areas of EFNB1-positive and EFNB1-negative cells. In contrast to the heterogeneous cell populations of heterozygotes, hemizygosity is characterized by a homogeneous cell population, in which ephrin-B1 may be replaced functionally by another B-class ephrin. This model is reminiscent of the concept of metabolic interference that has been proposed on theoretic grounds by Johnson (1980). Accordingly, the interaction of a mutant and a normal allele would lead to a more severe disturbance than the mutant allele alone. However, we propose the term "cellular interference" for what occurs between EphB-receptor–positive migrating cells and the two kinds of cell populations in heterozygotes, that is, cells with the active mutant X chromosome and cells with the active wild-type X chromosome. The experiments of Compagni et al. (2003) support this concept. Using the X-green fluorescence protein transgene for visualization of cells with the active wild-type X chromosome, they showed that ephrin-B1–positive and ephrin-B1–negative cells are organized in compartments by a random X inactivation. These compartments obviously exhibit different attractive impulses for invading EphB-receptor–positive cells.

In summary, we have demonstrated that mutations of *EFNB1* cause CFNS. For the first time, it can be shown that mutations of the ephrin receptor/ephrin signal transduction system are associated with a Mendelian disorder and that ephrin signaling is involved in human skeletal development. Finally, we propose an explanation of the sex-dependent manifestation of CFNS. The question of whether mutations in other ephrins, in their receptors, or in members of the signaling cascade may cause syndromes related to CFNS needs to be investigated.

Acknowledgments

Electronic-Database Information

Accession numbers and URLs for data presented herein are as follows:

Ensembl Genome Server, http://www.ensembl.org (for *EFNB1* [accession number ENSP00000204961])

GenBank, http://www.ncbi.nlm.nih.gov/Genbank (for *EFNB1* reference sequence [accession number XM_038809])

LocusLink, http://www.ncbi.nlm.nih.gov/LocusLink (for *EFNB1* [accession number 1947])

NCBI Molecular Variation Database (dbSNP), http://www.ncbi.nlm.nih.gov/SNP

Online Mendelian Inheritance in Man (OMIM), http://www.ncbi.nlm.nih.gov/Omim

References

Allen RC, Zoghbi HY, Moseley AB, Rosenblatt HM, Belmont JW (1992) Methylation of the HpaII and HhaI sites near the polymorphic CAG repeat in the human androgen-receptor gene correlates with X chromosome inactivation. Am J Hum Genet 51:1229–1239

Carrel L, Cottle A, Goglin KC, Willard HF (1999) A first-generation X-inactivation profile of the human X chromosome. Proc Natl Acad Sci 96:14440–14444

Compagni A, Logan M, Klein R, Adams R (2003) Control of skeletal patterning by EphrinB1-EphB interactions. Dev Cell 5:217–230

Devriendt K, van Mol C, Fryns JP (1995) Craniofacial dysplasia: a more severe expression in the mother than in her son. Genet Couns 6:361–364

Feldman GJ, Ward DE, Lajeunie-Renier E, Saavedra D, Robin NH, Proud V, Robb LJ, Der Kaloustian V, Carey JC, Cohen M, Cornier V, Munnich A, Zackai EH, Wilkie AOM, Price RA, Muenke M (1997) A novel phenotypic pattern in X-linked inheritance: craniofrontonasal syndrome maps to Xp22. Hum Mol Genet 6:1937–1941

Henkemeyer M, Orioli D, Henderson JT, Saxton TM, Roder J, Pawson T, Klein R (1996) Nuk controls pathfinding of commissural axons in the mammalian central nervous system. Cell 86:35–46

Himanen J-P, Rajashankar KR, Lackmann M, Cowan CA, Henkemeyer M, Nikolov DB (2001) Crystal structure of an Eph receptor-ephrin complex. Nature 414:933–938

Johnson WG (1980) Metabolic interference and +-heterozygote: a hypothetical form of simple inheritance which is neither dominant nor recessive. Am J Hum Genet 32:374–386

Koolpe M, Dail M, Pasquale EB (2002) An ephrin mimetic peptide that selectively targets the EphA2 receptor. J Biol Chem 277:46974–46979

Kullander K, Klein R (2002) Mechanisms and functions of Eph and ephrin signalling. Nat Rev Mol Cell Biol 3:475–486

Murai KK, Pasquale EB (2003) "Eph"ective signaling: forward, reverse and crosstalk. J Cell Science 116:2823–2832

Orioli D, Henkemeyer M, Lemke G, Klein R, Pawson T (1996) Sek4 and Nuk receptors cooperate in guidance of commissural axons and in palate formation. EMBO J 15:6035–6049

Saavedra D, Richieri-Costa A, Guion-Almeida ML, Cohen M (1996) Craniofrontonasal syndrome: study of 41 patients. Am J Med Genet 61:147–151

Sambrook J, Fritsch EF, Maniatis T (1989) Molecular cloning: a laboratory manual, 2nd ed. Cold Spring Harbor Laboratory Press, Cold Spring Harbor, NY

Toth J, Cutforth T, Gelinas AD, Bethoney KA, Bard J, Harrison CJ (2001) Crystal structure of an ephrin ectodomain. Dev Cell 1:83–92

Wieland I, Jakubiczka S, Muschke P, Wolf A, Gerlach L, Krawczak M, Wieacker P (2002) Mapping of a further locus for X-linked craniofrontonasal syndrome. Cytogenet Genome Res 99:285–288

Wilkinson DG (2001) Multiple roles of EPH receptors and ephrins in neural development. Nat Rev Neurosci 2:155–164